Journal of Physics: Conference Series **131** (2008) 012003 doi:10.1088/1742-6596/131/1/012003

Testing for periodicities in near-IR light curves of Sgr A*

Tuan Do[1], Andrea M Ghez[1], Mark R Morris[1], Sylvana Yelda[1], Jessica R Lu[1], Seth D Hornstein[2] and Keith Matthews[3]

[1]Physics and Astronomy Department, Los Angeles, CA 90095-1547
[2]Center for Astrophysics and Space Astronomy, Department of Astrophysical and Planetary Sciences, University of Colorado, Boulder, CO 80309
[3]California Institute of Technology, Pasadena, CA

E-mail: tdo@astro.ucla.edu

Abstract. We present the results of near-infrared (2 μm) monitoring of Sgr A*-IR with 1 minute time sampling using laser guide star adaptive optics (LGS AO) system at the Keck II telescope. Sgr A*-IR was observed continuously for up to three hours on each of seven nights, between 2006 May and 2007 August. Sgr A*-IR is detected at all times and is continuously variable. These observations allow us to investigate Nyquist sampled periods ranging from about 2 minutes to an hour. Of particular interest are periods of ∼20 min, which corresponds to a quasi-periodic (QPO) signal claimed based upon previous near-infrared observations and interpreted as the orbit of a 'hot spot' at or near the last stable orbit of a spinning black hole. We investigate these claims by comparing periodograms of the light curves with models for red noise and find no significant deviations that would indicate QPO activity at any time scale probed in the study. We find that the variability of Sgr A* is consistent with a model based on correlated noise with a power spectrum having a frequency dependence of $\sim f^{-2.5}$, consistent with that observed in AGNs. Furthermore, the periodograms show power down to the minimum sampling time of 2 min, well below the period of the last stable orbit of a maximally spinning black hole, indicating that the Sgr A*-IR light curves observed in this study is unlikely to be from the Keplerian motion of a single 'hot spot' of orbiting plasma.

1. Introduction

The existence of a super-massive black hole with a mass of $\sim 4 \times 10^6 M_\odot$ at the center of the Galaxy has now been firmly established from monitoring the orbits of the stars in the near-infrared (NIR) within 1 arcsecond of the location of the associated radio source Sgr A* [e.g. 1–4]. Multi-wavelength detections of the radio point source at sub-millimeter, X-ray, and infrared wavelengths have also been made, showing that the luminosity associated with the black hole is many orders of magnitudes below that of active galactic nuclei (AGN) with comparable masses [5]. These observations have also shown that the emission from Sgr A* is variable [e.g., 6–10]. Although it is now easily detected in its bright states when its flux increases by up to an order of magnitude over time scales of 1 to 3 hours, Sgr A* is difficult to detect in its faintest states at X-ray wavelengths because of the strong diffuse background, and in the near-infrared because of confusion with nearby stellar sources [6, 9]. Advances in adaptive optics (AO) technology have offered improved sensitivity to infrared emission from Sgr A* against the stellar background, such that observations in its faint states are now possible [11].

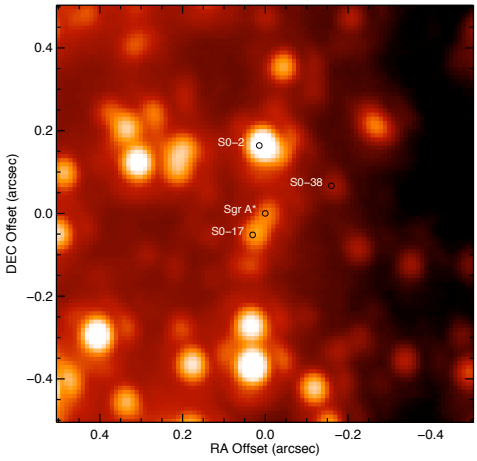

Figure 1. A K' image from 2006 May 3 of the central 0.″5 around Sgr A* with a logarithmic intensity scale so that the faint sources can be more easily seen. Sgr A* is in the center of the image along with the comparison stars, S0-2, S0-17 and S0-38. The image is oriented with north up and east to the left, with offsets in projected distance from Sgr A*.

At both NIR and X-ray wavelengths, a possible quasi-periodic oscillation (QPO) signal with a $\sim$ 20 min period has been reported in light curves of Sgr A* [12–14]. Models that aim to produce QPO signals include both a class of models involving the Keplerian orbits of 'hot spots' of plasma at the last stable orbit [15, 16] as well as the result of rotational modulations of instabilities in the accretion flow [17]. Since the orbital period at the last stable orbit of a non-spinning black hole is longer than 20 min, this putative periodic signal has been interpreted as evidence for a spinning black hole. The challenges for these claims are the relatively short time baselines of the observations (only a few times the claimed period), the low amplitude of the possible QPO activity, and the lack of rigorous assessment of the statistical significance of the claimed periodicity.

An alternative explanation for peaks in the periodograms seen in previous studies and interpreted as a periodic signal is that they are a sign of a frequency dependent physical process, commonly known as red noise [18]. The power spectrum of such a physical process will display an inverse power law dependence on frequency, which will result in light curves with large amplitude variations over long time scales and small amplitude variations over short time scales. The power spectrum of any individual realization of a red noise light curve will show statistical fluctuations around the intrinsic power law function, creating spurious peaks leading to an interpretation of periodic activity. Variability studies of other accreting black hole systems like AGNs and Galactic X-ray binaries have shown that their power spectral densities are consistent with red noise. Several physical models have been proposed that produces red noise light curves from AGNs [e.g. 19–21]; one common model that produces a red noise spectrum is from fluctuations in the physical parameters, such as the gas densities and accretion rate, at different radii of a turbulent magnetohydrodynamic accretion disk [22]. While QPO signals have been unambiguously confirmed in X-ray binaries, no QPO signals in AGNs have been shown to be statistically different than red noise [23, 24]. Recent re-analysis of X-ray light curves of Sgr A*, when including the contribution from red noise, show no indications of a QPO signal [25].

2. Observations and Data Reduction

The Galactic center has been extensively imaged between 2005 and 2007 with the Keck II 10 m telescope using the laser guide star adaptive optics (LGS AO) [26, 27] system and the NIRC2 near infrared camera (P.I. K. Matthews). For this study we include all nights of LGS-AO observations at K' (2 μm) that had sampling of 1-3 minutes, a total time baseline of more than

Table 1. Summary of Sgr A* Observations

Date (UT)	N_{obs}	Duration (min)	Dither	Strehl (%)	FWHM (mas)	Mean Flux (mJy)	σ (mJy)
2006 May 03	116	140	Yes	34	60	0.29	0.15
2006 June 20	109	125	Yes	24	71	0.24	0.18
2006 June 21	164	164	Yes	33	61	0.19	0.07
2006 July 17	70	189	No	35	59	0.15	0.05
2007 May 18	77	84	Yes	36	59	0.29	0.14
2007 August 12	62	57	Yes	33	58	0.16	0.02

1 hour, and at least 60 data points. As summarized in Table 1, this resulted in a selection of data sets with durations ranging from 80 min to 3 hours.

A detailed description of LGS AO observations of the Galactic center are described in [11]; here, we only summarize the setup specific to our observations. Images were obtained using the K' band-pass filter (λ_o = 2.12 μm,Δ λ = 0.3 μm) and were composed of 10 coadded 2.8 sec exposures, for a total integration time of 28 sec. For five nights, the time interval between each image is about 50 seconds, with dithers every three minutes. K' images from 2006 July 17 were sampled at 3 minute intervals but were not dithered. On average, the Strehl ratio was 32%, with a full width of the core at half-maximum intensity (FWHM) of $\sim$ 60 mas as measured from the relatively isolated star IRS 33N.

Photometry was performed on the individual images using the point spread function (PSF) fitting program *Starfinder* [28]. The program was enhanced as described in [9] to include the *a priori* knowledge of the location of Sgr A* and nearby sources in order to facilitate the detection of Sgr A* at faint flux levels in these short exposures. To do this, for each night of observation, the position of Sgr A*-IR and nearby sources was determined in a nightly-averaged image produced by a weighted average of individual images from that night (see Figure 1). We then use this knowledge of the location of all the sources as fixed inputs into *Starfinder* to more accurately fit for the flux contribution of sources near Sgr A* in the individual short exposure images. We also include only images with Strehl ratios greater than 20% to minimize large errors in the photometry from bad seeing conditions, which resulted in dropping only about 10 data points out of all nights. We are able to detect Sgr A* at all times, even at its faintest flux levels. The gaps in the data are from technical disruptions in the observations.

Photometric calibrations were performed relative to the list of non-variable sources from [29] at K'. The photometric error at each flux density level seen in Sgr A* was estimated by fitting a power law to the rms uncertainty in the flux for all non-variable stars in the same range of brightnesses observed for Sgr A* within 0.″5 of the black hole. The flux measurement uncertainties are comparable for all nights except 2006 June 20, the night with the worst seeing. Within the range of observed Sgr A* fluxes, we are on average able to achieve between 3 to 15% relative photometric precision for each 28 sec K' exposure. A source of systematic error in the flux measurements is the proximity of Sgr A* to unresolved sources, which would contribute flux. This contribution is only likely to have an impact when Sgr A* is faint [9], but for the purpose of this variability study, this effect is likely only a systematic offset in the mean flux density and as a source of white noise. For comparison to Sgr A*, we also present the light curves of the nearby stars S0-17 and S0-38. S0-17 (K' = 15.5 mag) was chosen because it is spatially closest to Sgr A*, with a projected distance from Sgr A* of $\sim$ 56 mas in 2006 May

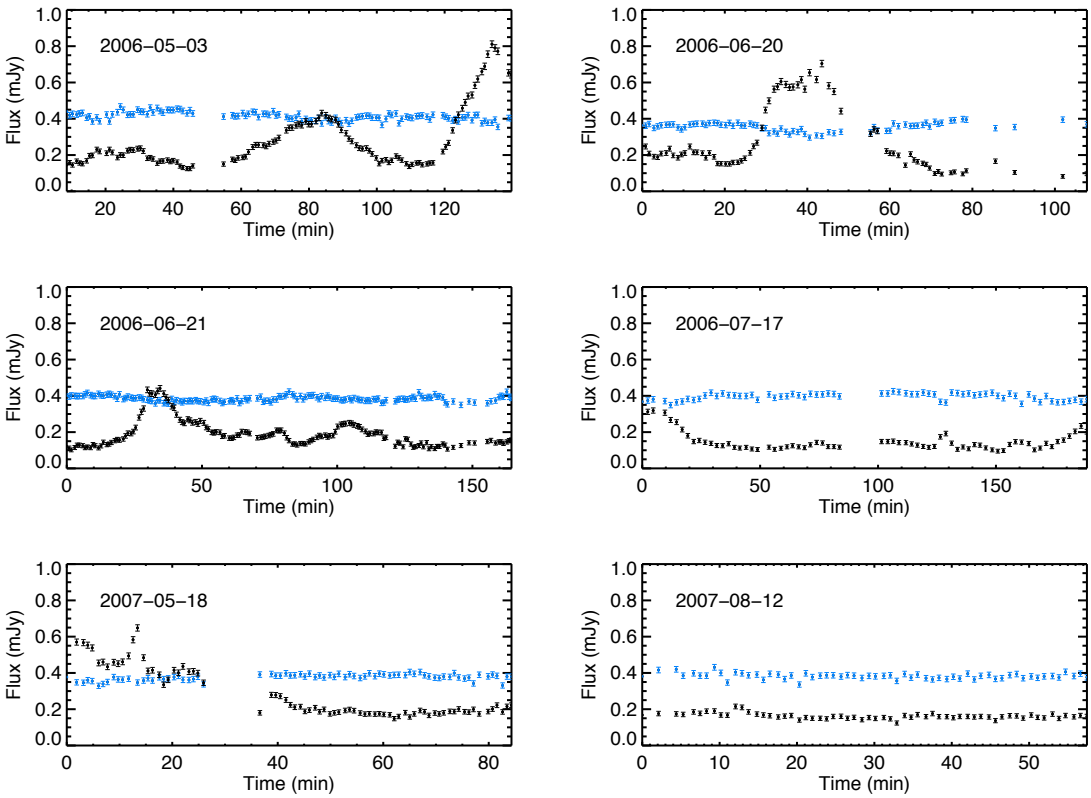

Figure 2. Sgr A* light curves (black) at K' with the star S0-17 (blue) for comparison.

to $\sim$ 48 mas in 2007 August; monitoring S0-17 is helpful to ensure that the variations in flux seen in Sgr A* are not a systematic effect of seeing or bias from nearby sources. The star S0-38 ($K' \sim 17$), $\sim 0''.2$ from Sgr A*, was chosen as a stellar reference because it has a similar flux to the faintest observed emission from Sgr A*. Figure 1 shows an image of this region and the location of the comparison sources with respect to Sgr A*. Unless otherwise stated, the fluxes in this paper are observed fluxes and not corrected for extinction to Sgr A*.

3. Results and Analysis

3.1. Light Curves and Timing Analysis

Figure 2 shows the resulting light curves for Sgr A* and a non-variable comparison source for each night of observation. While comparison sources show no significant time variable emission, Sgr A* shows variations on time scales ranging from minutes to hours, with peak emission that can be 10 times higher than during its faintest states. The emission peaks, or 'flares', are time symmetric, with similar rise and fall times.

3.1.1. Periodogram It is important to consider all possible sources of noise when testing for periodicity in light curves. While peaks in the periodograms are a good place to start searching for periodicity, the peaks must have significantly more power than those produced by non-periodic processes to be unambiguously attributed to a true periodicity in any variable source. White (Gaussian) noise processes are unlikely to lead to large peaks in the periodograms because they contribute equal power at all frequencies. However, time-correlated physical processes can

result in variability that is frequency dependent. One common variability characteristic - often seen in AGN light curves - is red noise, which can lead to spurious signals in a power spectrum or periodogram from a data set having a time baseline only a few times longer than that of the putative period, since it will show large amplitude fluctuations at low frequencies and small amplitudes at high frequencies. This can lead to relatively large stochastic peaks in the power spectrum at low frequencies, far above what would be expected from white noise. We emphasize that, although the term for this type of power law dependence of the flux variability is 'red noise', this variability arises from physical processes from the source and is not a result of measurement uncertainties such as Poisson noise, which behaves like white noise in its power spectrum.

One of the goals in this timing analysis is to test whether a purely red noise model can explain the variability of Sgr A*. The PSD of a red noise light curve is a power law, with greater power at lower frequencies: $P(\omega) \equiv f^{-\alpha}$, where f is the frequency and α is the power law index. For example, $\alpha = 0$ for white noise and $\alpha = 1$ for classical flicker noise [18]. All red noise simulations in this paper were produced by an algorithm detailed in [30], which randomizes both phase and amplitude of an underlying power law spectrum and then inverse Fourier transforms it into the time domain to create light curves. Our procedure for producing simulated light curves is as follows: first, a light curve is produced from a PSD with a specific power law slope evenly sampled at half the shortest observed time sampling interval; we then re-sample the light curve at the exact sampling times used during the specific night that we are simulating; finally, since the simulation has an arbitrary flux scale, we scale the light curves to have the same mean and standard deviation as that night.

Instead of computing the PSD, which is often used for evenly sampled data, we searched for periodicity by computing a related function for unevenly sampled data: the normalized Lomb-Scargle periodogram [31]; given a set of data values h_i, $i = 1, \ldots, N$ at times t_i the periodogram is defined as:

$$P_N(\omega) \equiv \frac{1}{2\sigma^2} \left\{ \frac{[\sum_j (h_j - \overline{h}) \cos \omega(t_j - \tau)]^2}{\sum_j \cos^2 \omega(t_j - \tau)} + \frac{[\sum_j (h_j - \overline{h}) \sin \omega(t_j - \tau)]^2}{\sum_j \sin^2 \omega(t_j - \tau)} \right\} \quad (1)$$

where ω is the angular search frequency, $\overline{h}$ and σ^2 are the mean and variance of the data respectively. The constant τ is an offset introduced to keep the periodogram phase invariant:

$$\tan(2\omega\tau) = \frac{\sum_j \sin 2\omega t_j}{\sum_j \cos 2\omega t_j} \quad (2)$$

Since the periodogram is normalized by the variance of the flux, a light curve consisting of only white noise, or equivalently, red noise with a power law $\alpha = 0$, will have an average power of 1 at all frequencies.

The normalized Lomb-Scargle periodogram was computed for each light curve, oversampled by a factor of 4 times the independent Fourier intervals in order to increase the sensitivity to periods between the Fourier frequencies (Figure 3). Assuming that the physical source of the variability is stationary, we averaged together the periodograms for the five K' nights which have durations longer than 80 minutes (Figure 3.1.1). The combined periodogram excludes the 2007 August 12 night because it is less than an hour long, leading to poor sampling at low frequencies compared to the other nights. The combined periodogram is consistent with red noise, except for the peak corresponding to the time scale of the three minute dithers. To characterize the underlying spectrum, we have performed Monte Carlo simulations combining red noise light curves with the same sampling as the data set. We tested several different underlying PSD and found that the combined periodogram is consistent with a power law index of 2.5, with no periodic components. This model is able to reproduce the slope of the periodogram, the increase in power at three minutes from dithering, and the flattening of the periodogram at

very low frequencies caused by poor sampling at those frequencies. Figure 3.1.1 shows the results of Monte Carlo simulations with power law indices 1.5, 2.0, 2.5, and 3.0. The simulations shows that the resulting periodograms tend to be flatter than the intrinsic PSD because the limited time sampling at low frequencies results in poor sensitivity to long time scale variations characteristic of steeper power laws. We find that this effect is especially pronounced for $\alpha > 2$, which suggests that we have a better constraint on the lower limit than on the upper limit to our estimate for the slope of the PSD.

Although there is no evidence for QPO activity in the combined periodogram, we would like to test the case for a transient QPO phenomenon in each night. We therefore used our best fit of $\alpha = 2.5$ for the power law of the combined periodogram to test each night for statistically significant deviations from a purely red noise model. Our criterion for a statistically significant peak in the periodogram is that its power must be above the 99.7% (3σ) confidence interval from a Monte Carlo simulation with 10^5 realizations of red noise light curves. This method of establishing the significance of peaks in the periodogram is similar to the one proposed by [24] for evenly sampled data, but modified here to account for our unevenly sampled data set by using the Lomb-Scargle periodogram instead of the Fourier transform. The resulting periodograms are shown in figure 3. The individual periodograms show peaks at low frequencies, but these appear to be consistent with red noise, with no peaks having power greater than the 3σ threshold derived from the Monte Carlo simulations. We have also repeated the same procedure for power law indices between 1.0 and 3.0 with the same result.

By adding an artificial sinusoidal periodic signal to the red noise simulations, we can address the sensitivity for detecting QPOs in the presence of red noise. In order to test this, a periodic sinusoidal signal was introduced into a simulated light curve with a red noise PSD slope of 2.5. The amplitude of the periodic signal was increased until the periodogram showed a peak at the frequency of the input signal above the previously determined 3σ threshold. For example, for the time sampling and duration corresponding to the observations on 2006 May 3, we find that we are able to detect a 20 min periodic signal with an amplitude that is 20% of the maximum flux seen in Sgr A* on that night. The sensitivity for the detection of a QPO increases with frequency because the underlying red noise component has less power at higher frequencies (e.g. a 10 (40)-minute QPO signal will result in power greater than expected from red noise when its amplitude is 5% (30%) of the maximum flux density). Our sensitivity for the detection of a periodic signal is similar for the other observed light curves with similar durations (> 2 hours). Note that attempting to remove the flares with a low-order functional fit to increase sensitivity to periodic signals will introduce a statistical bias, because that will only remove some combination of low frequency power without actually removing the red noise component. Because the light curves are consistent with a red noise process at all timescales, including the flares, any statistical analysis must be performed without first modifying the light curves.

4. Discussion and Conclusion

Our analysis shows that the Sgr A* near-infrared light curves observed in this study are entirely consistent with red noise and no evidence for a QPO signal near 20 min (or any other time scale) is seen. In addition, power seen at the shortest time scales measured in the periodogram (2 min), well below the orbital period at the last stable circular orbit of a spinning black hole ($\sim$ 5–30 min), indicates that the high frequency variability is not simply from Keplerian motion of a single orbiting 'hot spot', leading to flux modulations observed as the IR flares [15, 16]. The high frequency variability must originate from small areas of the accretion flow. In addition to power at high frequencies, the light curve for 2007 May 18 shows a strong spike in flux at about 10 min with a duration of ~ 5 min, and a rise time of only ~ 3 min, which also suggests that regions of the accretion flow responsible for the variability can be as small as 0.4 AU.

It is important to note that the significance threshold used in this study tests whether the

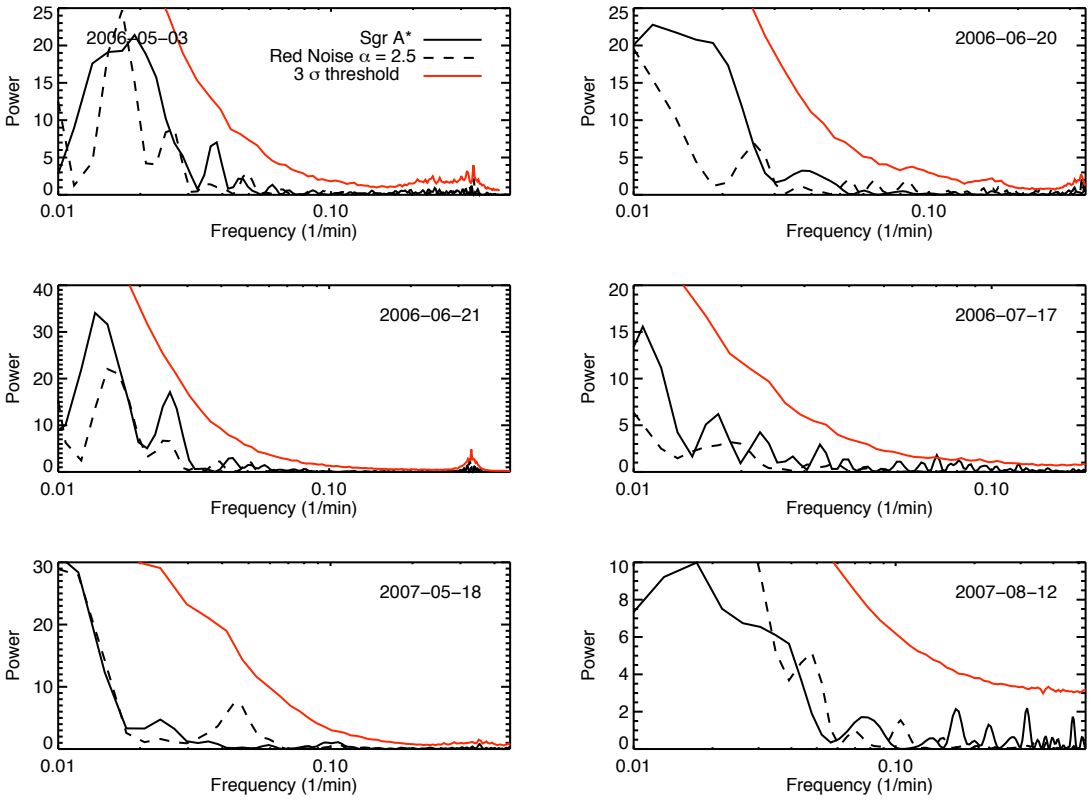

Figure 3. Normalized Lomb-Scargle periodograms of the Sgr A* light curves (black) at K'. Plotted in red is the 3 σ significance threshold determined from Monte Carlo simulations of red noise with a power law index, $\alpha = 2.5$. The periodogram of a single realization of a $\alpha = 2.5$ red noise light curve at the same time sampling is also shown for comparison (dashed line).

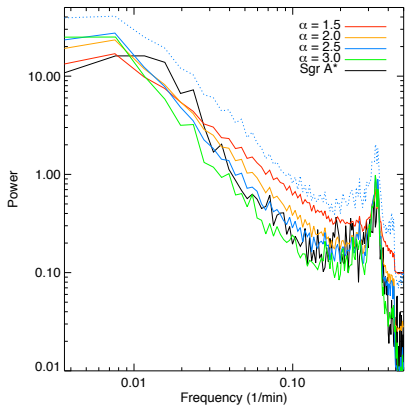

Figure 4. Combined periodogram from 5 nights of K' observations (black line). Colored lines are the average of 10^4 Monte Carlo simulations of combining data sets with the same sampling, for three different red noise power laws. The dotted blue line corresponds to the 3 σ threshold of power for red noise with $\alpha = 2.5$. The large spike at three minutes is an artifact resulting from the regular dithers in the observations.

periodogram power of peaks exceeds 3σ *at a given frequency*. It does not take into account that we are scanning over a large range of frequencies. If one searches enough frequencies, a peak of arbitrary power will appear at a random frequency. If a peak in the periodogram was found in this study that may indicate a periodic signal, then additional simulations should be performed to determine its statistical significance by accounting for the range of frequencies probed. This is referred to as the false alarm probability in [32] and has been calculated analytically for the case of white noise. In the case of red noise, the additional simulations would also need to account for the fact that larger peaks are more likely at low frequencies.

Acknowledgments
The infrared data presented herein were obtained at the W. M. Keck Observatory, which is operated as a scientific partnership among the California Institute of Technology, the University of California and the National Aeronautics and Space Administration. The Observatory was made possible by the generous financial support of the W. M. Keck Foundation. The authors wish to recognize and acknowledge the very significant cultural role that the summit of Mauna Kea has always had within the indigenous Hawaiian community. We are most fortunate to have the opportunity to conduct observations from this mountain.

References

[1] Schödel R, Ott T, Genzel R, Hofmann R, Lehnert M, Eckart A, Mouawad N, Alexander T, Reid M J, Lenzen R, Hartung M, Lacombe F, Rouan D, Gendron E, Rousset G, Lagrange A M, Brandner W, Ageorges N, Lidman C, Moorwood A F M, Spyromilio J, Hubin N and Menten K M 2002 Nature **419** 694–696 (*Preprint* `arXiv:astro-ph/0210426`)

[2] Schödel R, Ott T, Genzel R, Eckart A, Mouawad N and Alexander T 2003 ApJ **596** 1015–1034 (*Preprint* `arXiv:astro-ph/0306214`)

[3] Ghez A M, Duchêne G, Matthews K, Hornstein S D, Tanner A, Larkin J, Morris M, Becklin E E, Salim S, Kremenek T, Thompson D, Soifer B T, Neugebauer G and McLean I 2003 ApJ **586** L127–L131 (*Preprint* `arXiv:astro-ph/0302299`)

[4] Ghez A M, Salim S, Hornstein S D, Tanner A, Lu J R, Morris M, Becklin E E and Duchêne G 2005 ApJ **620** 744–757 (*Preprint* `arXiv:astro-ph/0306130`)

[5] Melia F and Falcke H 2001 ARA&A **39** 309–352 (*Preprint* `arXiv:astro-ph/0106162`)

[6] Baganoff F K, Maeda Y, Morris M, Bautz M W, Brandt W N, Cui W, Doty J P, Feigelson E D, Garmire G P, Pravdo S H, Ricker G R and Townsley L K 2003 ApJ **591** 891–915 (*Preprint* `arXiv:astro-ph/0102151`)

[7] Mauerhan J C, Morris M, Walter F and Baganoff F K 2005 ApJ **623** L25–L28 (*Preprint* `arXiv:astro-ph/0503124`)

[8] Eisenhauer F, Genzel R, Alexander T, Abuter R, Paumard T, Ott T, Gilbert A, Gillessen S, Horrobin M, Trippe S, Bonnet H, Dumas C, Hubin N, Kaufer A, Kissler-Patig M, Monnet G, Ströbele S, Szeifert T, Eckart A, Schödel R and Zucker S 2005 ApJ **628** 246–259 (*Preprint* `arXiv:astro-ph/0502129`)

[9] Hornstein S D, Matthews K, Ghez A M, Lu J R, Morris M, Becklin E E, Rafelski M and Baganoff F K 2007 ApJ **667** 900–910 (*Preprint* `arXiv:0706.1782`)

[10] Marrone D P, Baganoff F K, Morris M, Moran J M, Ghez A M, Hornstein S D, Dowell C D, Munoz D J, Bautz M W, Ricker G R, Brandt W N, Garmire G P, Lu J R, Matthews K, Zhao J , Rao R and Bower G C 2007 *ArXiv e-prints* **712** (*Preprint* `0712.2877`)

[11] Ghez A M, Hornstein S D, Lu J R, Bouchez A, Le Mignant D, van Dam M A, Wizinowich P, Matthews K, Morris M, Becklin E E, Campbell R D, Chin J C Y, Hartman S K, Johansson

E M, Lafon R E, Stomski P J and Summers D M 2005 ApJ **635** 1087–1094 (*Preprint* arXiv:astro-ph/0508664)

[12] Genzel R, Schödel R, Ott T, Eckart A, Alexander T, Lacombe F, Rouan D and Aschenbach B 2003 Nature **425** 934–937 (*Preprint* arXiv:astro-ph/0310821)

[13] Aschenbach B, Grosso N, Porquet D and Predehl P 2004 A&A **417** 71–78 (*Preprint* arXiv:astro-ph/0401589)

[14] Eckart A, Schödel R, Meyer L, Trippe S, Ott T and Genzel R 2006 A&A **455** 1–10 (*Preprint* arXiv:astro-ph/0610103)

[15] Meyer L, Eckart A, Schödel R, Duschl W J, Mužić K, Dovčiak M and Karas V 2006 A&A **460** 15–21 (*Preprint* arXiv:astro-ph/0610104)

[16] Trippe S, Paumard T, Ott T, Gillessen S, Eisenhauer F, Martins F and Genzel R 2007 MNRAS **375** 764–772 (*Preprint* arXiv:astro-ph/0611737)

[17] Falanga M, Melia F, Tagger M, Goldwurm A and Bélanger G 2007 ApJ **662** L15–L18 (*Preprint* arXiv:0705.0238)

[18] Press W H 1978 *Comments on Astrophysics* **7** 103–119

[19] Lyubarskii Y E 1997 MNRAS **292** 679–+

[20] Armitage P J and Reynolds C S 2003 MNRAS **341** 1041–1050 (*Preprint* arXiv:astro-ph/0302271)

[21] Vaughan S, Fabian A C and Nandra K 2003 MNRAS **339** 1237–1255 (*Preprint* arXiv:astro-ph/0211421)

[22] Kataoka J, Takahashi T, Wagner S J, Iyomoto N, Edwards P G, Hayashida K, Inoue S, Madejski G M, Takahara F, Tanihata C and Kawai N 2001 ApJ **560** 659–674 (*Preprint* arXiv:astro-ph/0105022)

[23] Benlloch S, Wilms J, Edelson R, Yaqoob T and Staubert R 2001 ApJ **562** L121–L124 (*Preprint* arXiv:astro-ph/0110204)

[24] Vaughan S 2005 A&A **431** 391–403 (*Preprint* arXiv:astro-ph/0412697)

[25] Bélanger G, Terrier R, de Jager O C and Melia F 2008 in prep ApJ

[26] Wizinowich P L, Le Mignant D, Bouchez A H, Campbell R D, Chin J C Y, Contos A R, van Dam M A, Hartman S K, Johansson E M, Lafon R E, Lewis H, Stomski P J, Summers D M, Brown C G, Danforth P M, Max C E and Pennington D M 2006 PASP **118** 297–309

[27] van Dam M A, Bouchez A H, Le Mignant D, Johansson E M, Wizinowich P L, Campbell R D, Chin J C Y, Hartman S K, Lafon R E, Stomski Jr P J and Summers D M 2006 PASP **118** 310–318

[28] Diolaiti E, Bendinelli O, Bonaccini D, Close L, Currie D and Parmeggiani G 2000 A&AS **147** 335–346 (*Preprint* arXiv:astro-ph/0009177)

[29] Rafelski M, Ghez A M, Hornstein S D, Lu J R and Morris M 2007 ApJ **659** 1241–1256 (*Preprint* arXiv:astro-ph/0701082)

[30] Timmer J and Koenig M 1995 A&A **300** 707–+

[31] Press W H and Rybicki G B 1989 ApJ **338** 277–280

[32] Horne J H and Baliunas S L 1986 ApJ **302** 757–763